

Title	Dimethylamine borane oxidation for electroless deposition from alkaline solutions
Authors	Rohan, James F.;Ahern, Bernadette M.;Nagle, Lorraine C.
Publication date	2006-07
Original Citation	Rohan, J. F., Ahern, B. M. and Nagle, L. C. (2006) 'DMAB Oxidation for Electroless Deposition from Alkaline Solutions', ECS Transactions, 1(31), pp. 1-9. doi: 10.1149/1.2209381
Type of publication	Article (peer-reviewed)
Link to publisher's version	<a href="http://ecst.ecsdl.org/content/1/31/1">http://ecst.ecsdl.org/content/1/31/1</a> - 10.1149/1.2209381
Rights	© 2006 ECS - The Electrochemical Society
Download date	2024-12-02 17:13:46
Item downloaded from	<a href="https://hdl.handle.net/10468/7606">https://hdl.handle.net/10468/7606</a>



**UCC**

**University College Cork, Ireland**  
Coláiste na hOllscoile Corcaigh

# **Dimethylamine Borane Oxidation For Electroless Deposition From Alkaline Solutions.**

James F. Rohan, Bernadette M. Ahern and Lorraine C. Nagle.

Tyndall National Institute, National University of Ireland, Lee Maltings, Cork, Ireland.

Dimethylamine borane (DMAB) has been used as a reducing agent in electroless baths for many years. There has been an increased interest in DMAB-based electroless baths recently for applications in microelectronics such as barrier/capping layers for copper IC interconnect. To optimise the plating baths a thorough understanding of the role of each of the bath constituents is required. To this end we have employed microelectrodes to investigate the oxidation mechanism of boranes in alkaline solutions. In this paper we present data for DMAB and the simpler ammonia borane (AB) to assist in the analysis of borane oxidation in alkaline solutions. Both DMAB and AB are shown to oxidise in two steady state mass transport-controlled oxidation waves for specific concentration ranges. The potential range for oxidation, the optimum concentration and a suggested mechanism for oxidation are shown.

## **Introduction.**

The oxidation of amine boranes in aqueous solutions is increasingly being investigated to optimise the low cost deposition of materials such as metals [1-8], semiconductors [9, 10] and insulators [11] through electroless processing for microtechnology applications. Boranes and borohydrides have the additional advantage over the most widely used alternative reducing agent, hypophosphite, of being catalytically oxidised at technologically significant substrates such as copper without the requirement for substrate palladium activation [12] which reduces the number of processing steps and can aid selectivity where applicable. Boranes and borohydrides also offer a (non-toxic) alternative to formaldehyde and hydrazine. Furthermore, the boron content in deposits can be significantly lower than the phosphorus codeposit from hypophosphite based baths leading to purer deposits of the desired material. There has also been an increased activity in the analysis of boranes [13, 14] or borohydride materials as fuels for fuel cell systems [15-19]. In the optimisation of plating baths or catalysts for the fuel cell systems it is desirable to know the likely oxidation mechanism for the reducing agent or fuel material. The multielectron reactions that occur during the complete oxidation of boranes or borohydrides have complicated attempts to decipher the oxidation mechanism. A recent review of electroless deposition concluded that further analysis is required to study the reducing agent reactions [20]. This study is intended to provide additional parameter information through microelectrode analysis of the borane oxidation reactions with relevance to electroless deposition and fuel cell reactions.

Microelectrodes have inherent qualities that facilitate the acquisition of high quality data [21]. In the specific case of borane oxidation, simple, dilute solutions may be investigated and they have been shown to yield data undistorted by ohmic drop or

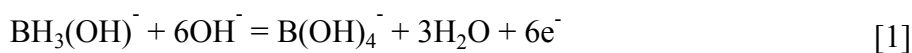
complications introduced by added electrolyte. Previous analysis in this laboratory [22] of the DMAB oxidation reaction at a gold microdisk in  $1 \text{ mol dm}^{-3}$  NaOH led to the determination of the diffusion coefficient and apparent coulomb number. The oxidation mechanism proposed therein made allowance for the possible complication of hydrogen gas evolution at lower ratios of hydroxide ion to borane. The microelectrode data indicated that for DMAB the oxidation proceeds via an irreversible three-electron oxidation followed by a second irreversible wave at more positive potentials of equal height and presumably equal electron transfer. The second wave was shown to be complicated by gold monolayer oxide and a true plateau was difficult to achieve. The first wave which occurs 500 mV more negative than the second wave has been attributed to the oxidation of an intermediate  $\text{BH}_3\text{OH}^-$  that does not appear to occur during the borohydride oxidation process in  $1 \text{ mol dm}^{-3}$  NaOH [23]. This apparent three-electron oxidation [22] is therefore in a more favourable potential region for electroless deposition given that the area of overlap of the oxidation and reduction reactions is significantly larger than for borohydride systems and would potentially lead to a cell voltage increase for fuel cells based on this system. We describe here the analysis of a simpler AB complex to probe the two-wave oxidation of the boranes and compare the oxidation behaviour with that of DMAB. The AB is itself a potential reducing agent/fuel for specific applications and the parameters determined in this work are necessary to assist in the characterisation of any system in which it is employed.

### **Experimental.**

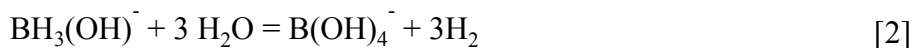
DMAB, AB (minimum purity 97 %) and sodium hydroxide (minimum purity 99 %) were purchased from Sigma Aldrich and used as received. Deionised water of resistivity  $18 \text{ M}\Omega \text{ cm}$  was used to prepare all solutions. The working electrode was a  $10 \mu\text{m}$  diameter Au microdisk (Princeton Applied Research) supplied by Advanced Measurement Technology, UK. This was polished with  $0.05 \mu\text{m}$  alumina powder obtained from Struers on a Buehler polishing cloth for 1-2 minutes and rinsed in deionised water. A  $0.5 \text{ mm}$  diameter Pt electrode of  $37 \text{ mm}$  length (IJ Cambria) was used as counter electrode. Cyclic voltammograms (CV) or linear sweep voltammograms (LSV) were recorded with respect to a Ag/AgCl, KCl saturated reference electrode (IJ Cambria). The potential of the working electrode was controlled using a CH Instruments potentiostat model 660B. The effective cell volume was  $20 \text{ ml}$ . All solutions were purged with nitrogen for 20 minutes prior to experiments in order to remove oxygen. All experiments were performed at  $20 \text{ }^\circ\text{C}$ .

### **Results and Discussion.**

Au microelectrodes in strongly alkaline solutions have been used to investigate the DMAB and AB oxidation mechanisms. Microelectrodes permit the analysis of dilute solutions without additional supporting electrolyte. In addition a negligible background current at Au in the potential region corresponding to borane oxidation also assists in this analysis. In strongly alkaline solution it is expected that DMAB [3,24-27], exists as the hydroxytrihydroborate ion,  $\text{BH}_3(\text{OH})^-$ , which may undergo oxidation with maximum coulombic efficiency on Au in base according to the reaction,



Competing chemical hydrolysis of AB with evolution of hydrogen, given by equation 2, is expected to be minimal in this solution [27].



Typical behaviour for gold in  $1\text{ mol dm}^{-3}$  NaOH is seen in the CV recorded over the potential range  $-1.15$  to  $+0.68$  V for a  $10\text{ }\mu\text{m}$  diameter microdisk electrode shown in Fig 1. This voltammogram shows that negligible current (subnanoamp) flows in the absence of DMAB over the potential range  $-1.15$  to  $+0.05$  V. The onset of monolayer oxide formation is shown to occur above  $+0.05$  V with the corresponding oxide reduction peak on the reverse sweep.

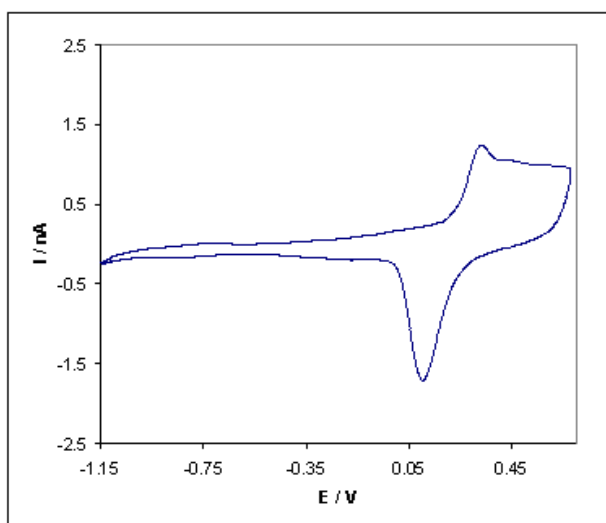


Figure 1. CV ( $-1.15$  to  $+0.68$  V) at Au microdisk in  $1\text{ mol dm}^{-3}$  NaOH at  $100\text{ mV s}^{-1}$ .

Upon addition of  $10\text{ mmol cm}^{-3}$  DMAB to the  $1\text{ mol dm}^{-3}$  solution of NaOH a well-defined CV (Fig. 2(a)) is achieved at a Au microdisk consisting of two irreversible anodic waves. Mass transport-controlled steady-state currents were recorded for the first wave at  $-0.65$  V and discussed in [22]. The oxidation exhibits complications in the second wave (shown in Fig. 3(a)) with the forward sweep giving a lower oxidation current than the reverse sweep. The proximity to the oxide region observed by a number of researchers [7,22,26] meant that this wave was not analysed in detail in the earlier analysis of DMAB oxidation at microelectrodes [22]. It should be noted however, that upon removal of the monolayer oxide the oxidation current almost achieves the same magnitude as the first wave. The reverse sweeps of the CVs are shown in Fig. 2(b) for a series of concentrations of DMAB. The steady state currents achieved are plotted in Fig 2(c). The linear nature of the current increase with increasing concentration on the reverse sweep is indicative of a mass transport controlled reaction for both waves. The data in Fig. 2(c) shows that the current achieved for the first wave is slightly higher than the second wave even when the data is taken from the reverse sweep.

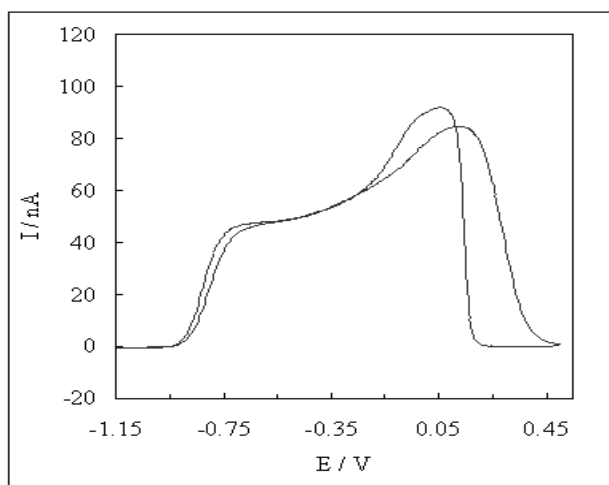


Figure 2(a). CV (-1.15 to 0.5 V) of  $10 \text{ mmol dm}^{-3}$  DMAB at Au microdisk in  $1 \text{ mol dm}^{-3}$  NaOH at  $100 \text{ mV s}^{-1}$ .

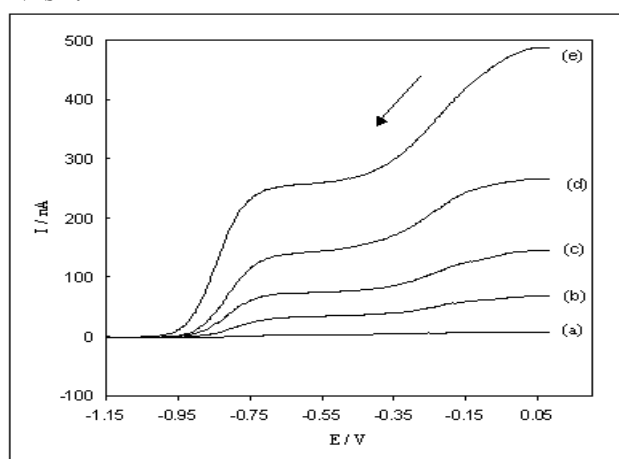


Figure 2(b). CV (-1.15 to 0.45 V) of DMAB (a) 0.9, (b) 8, (c) 17, (d) 36 and (e) 70  $\text{mmol dm}^{-3}$  at gold microdisk in  $1 \text{ mol dm}^{-3}$  NaOH at  $100 \text{ mV s}^{-1}$ . For clarity the data shown is the reverse sweep from 0.085 V to -1.15 V only.

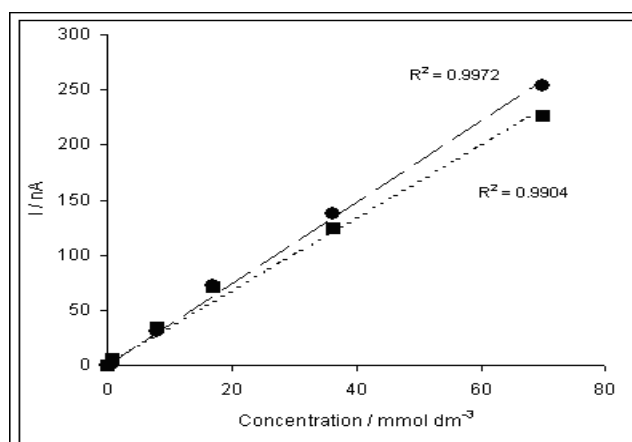


Figure 2(c) Plot of steady-state currents at  $\bullet$   $-0.65 \text{ V}$  and  $\blacksquare$   $0.0 \text{ V}$  (current at  $-0.65 \text{ V}$  subtracted) for DMAB at a gold microdisk in  $1 \text{ mol dm}^{-3}$  NaOH at  $100 \text{ mV s}^{-1}$ . Data is taken from the reverse sweep of the voltammograms.

The simpler ammonia borane was chosen to examine in more detail the oxidation reactions in alkaline solutions. When  $20 \text{ mmol dm}^{-3}$  AB is added to the  $1 \text{ mol dm}^{-3}$  NaOH solution a well-defined CV (Fig. 3(a)) is achieved at a Au microdisk consisting of two irreversible anodic waves. In this case mass transport-controlled steady-state currents were recorded for the first and second waves at  $-0.65 \text{ V}$  and  $-0.15 \text{ V}$ , respectively. The voltammograms exhibit a pronounced plateau region upon sweeping the potentials to more positive values unlike that observed for DMAB in the case of the second wave. The magnitude of the current for both anodic waves is equal and increases linearly with concentration of AB up to  $40 \text{ mmol dm}^{-3}$ , Figs. 3(b) and 3(c). The fit to the data shown in Fig. 3(c) indicates that unlike that observed for DMAB on the forward sweep the AB oxidation current increase in the second wave is linear with concentration added and not complicated by gold oxide behaviour at the electrode. When the AB concentration exceeded  $40 \text{ mmol dm}^{-3}$  the measured currents did not increase linearly with AB concentration and the reverse sweep did not retrace the forward sweep. In these cases the evolution of gas, presumably hydrogen, was obvious. The AB solution is a simpler system than DMAB with overlap of the oxidation current on the forward and reverse sweeps at potentials more negative than  $0.05 \text{ V}$ . It appears that the oxidation of DMAB is impeded by other species in addition to the complication caused by formation of gold monolayer oxide. In the oxidation wave of DMAB the forward and reverse currents start to diverge at potentials more positive than  $-0.25 \text{ V}$ . AB oxidation is not impeded in this way even on the forward sweep until approx  $+0.06 \text{ V}$  after which it is assumed the same surface oxide should be present in the otherwise identical electrolyte.

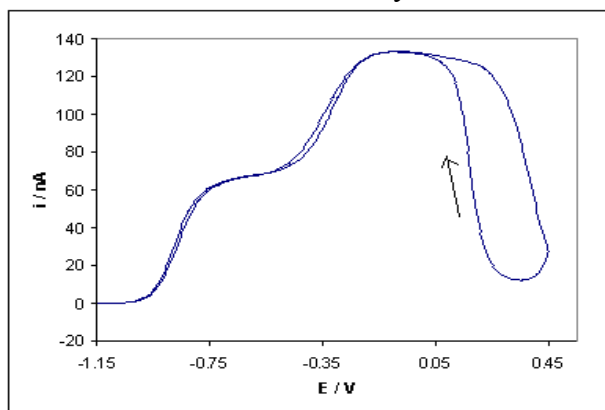


Figure 3(a). CV ( $-1.15$  to  $0.45 \text{ V}$ ) of  $20 \text{ mmol dm}^{-3}$  AB at Au microdisk in  $1 \text{ mol dm}^{-3}$  NaOH at  $100 \text{ mV s}^{-1}$ .

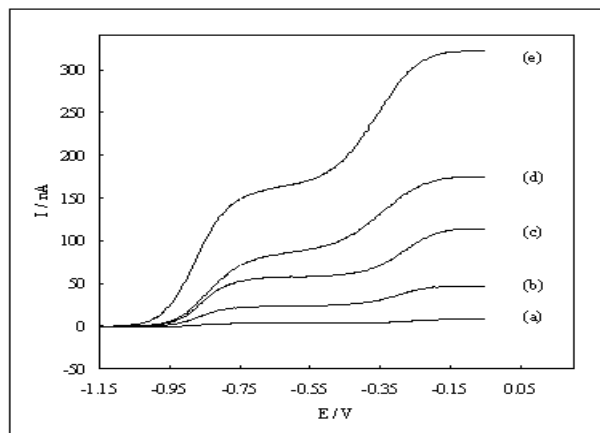


Figure 3(b). LSV ( $-1.15$  to  $-0.055 \text{ V}$ ) of AB (a)  $1.1$ , (b)  $7.2$ , (c)  $16.2$ , (d)  $20$  and (e)  $40 \text{ mmol dm}^{-3}$  at gold microdisk in  $1 \text{ mol dm}^{-3}$  NaOH at  $100 \text{ mV s}^{-1}$ .

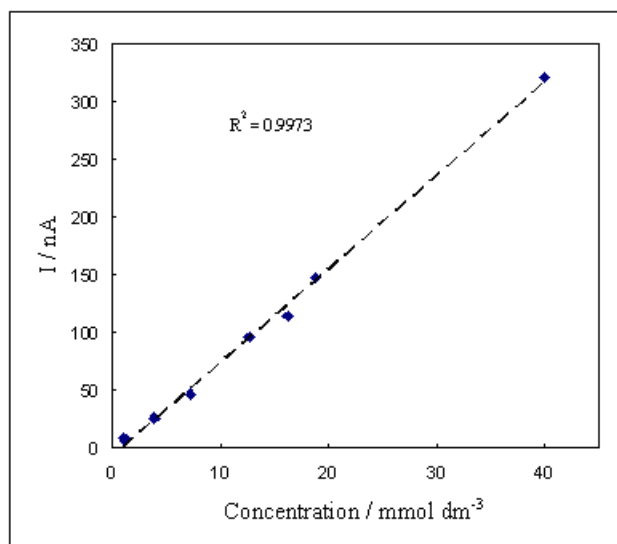


Figure 3(c). Plot of steady-state current at  $-0.15$  V for second oxidation wave vs. concentration for AB at gold microdisk in  $1 \text{ mol dm}^{-3}$  NaOH at  $100 \text{ mV s}^{-1}$

Dimethylamine was added to the solution to examine its possible influence on the reaction. The results are shown in Fig. 4. The gradual addition of dimethylamine to a  $10 \text{ mmol dm}^{-3}$  solution AB in  $1 \text{ mol dm}^{-3}$  NaOH results in a decrease in magnitude of the current for the second anodic wave and at very high concentrations the first wave is also influenced to an extent. The second oxidation wave for AB becomes drawn out and the plateau current becomes less obvious before the potential reaches the gold monolayer oxide region. This behaviour is observed on forward scans for solutions of DMAB. It is suggested that the dimethylamine has an influence on the borane oxidation reaction by non-Faradaic surface interactions at the electrode leading to a decrease in the magnitude of the second oxidation wave.

The oxidation of AB was further analysed to determine the diffusion coefficient in this medium using a technique introduced by Bard et al [27]. Microelectrodes enable the determination of the diffusion coefficient without a prior knowledge of  $n$ . The coulomb number has not been previously demonstrated and hence this analysis is required to extract the unknown parameters. As stated earlier, the diffusing species in this  $1 \text{ mol dm}^{-3}$  NaOH solution is likely to be  $\text{BH}_3\text{OH}^-$ . The diffusion coefficient was determined directly by analysing the chronoamperometric response for the first anodic wave which reaches a steady state at  $-0.65$  V. The current transient in response to a potential step from  $-1.15$  to  $-0.65$  V was recorded for  $20 \text{ mmol dm}^{-3}$  AB in  $1 \text{ mol dm}^{-3}$  NaOH. The  $D$  value determined is  $8.45 \times 10^{-6} \text{ cm}^2 \text{ s}^{-1}$ . This is similar to the value determined for DMAB ( $7.48 \times 10^{-6} \text{ cm}^2 \text{ s}^{-1}$ ) in an identical electrolyte [22]. It remains considerably lower than the value estimated by Bard et al [27] ( $1.68 \times 10^{-5} \text{ cm}^2 \text{ s}^{-1}$ ) for the  $\text{BH}_4^-$  species in the borohydride analysis

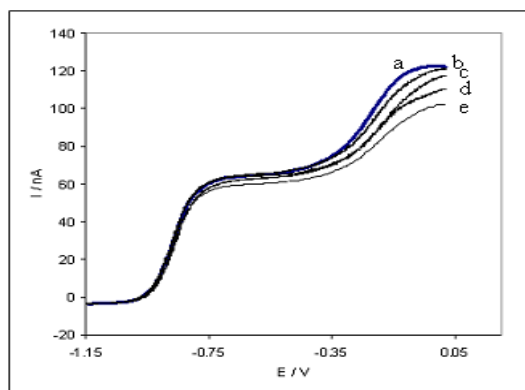


Figure 4. CV (-1.15 to -0.02 V) of 10 mmol dm<sup>-3</sup> AB with (a) 0, (b) 10, (c) 30 (d) 100 and (e) 200 mmol dm<sup>-3</sup> dimethylamine added at gold microdisk in 1 mol dm<sup>-3</sup> NaOH at 100 mV s<sup>-1</sup>.

Using the expression for the limiting current,  $I$ , under mass transport-controlled, steady state conditions at a microdisk electrode (equation 3) and  $8.45 \times 10^{-6} \text{ cm}^2 \text{ s}^{-1}$  for  $D$ , the coulomb number,  $n$ , was found to be 3.3.

$$I = 4nFDrC \quad [3]$$

where  $r$  is microdisk radius and  $C$  is concentration of AB.

It is assumed here that the diffusion coefficient for both oxidation waves represented in Fig. 3(a) is the same. Hence, given that the oxidation current associated with the first and second stages is equal, a value of three for  $n$  has also been assigned to the second oxidation stage, implying a total six-electron loss for AB oxidation. It has been noted previously by other workers that in solutions where  $\text{BH}_4^-$  hydrolysis had occurred [24,25,28] oxidation waves separated by 500 mV could be attributed to  $\text{BH}_3\text{OH}^-$  and  $\text{BH}_4^-$  oxidation. This separation is shown in Fig. 5 for solutions of AB, DMAB and  $\text{NaBH}_4$ . The currents achieved for  $\text{BH}_4^-$  oxidation are higher for smaller concentrations. This is most likely a result of the faster diffusion of the  $\text{BH}_4^-$  [23,27] by comparison with  $\text{BH}_3\text{OH}^-$  [22].

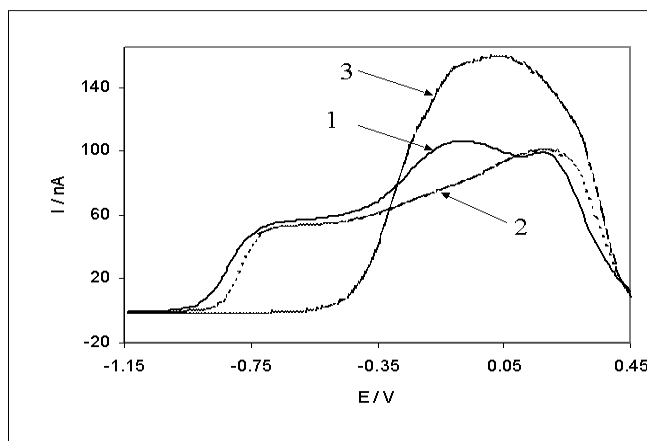
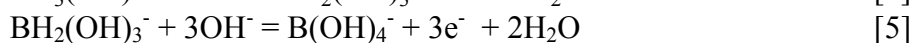
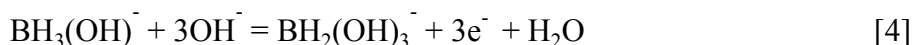


Figure 5. LSV (-1.15 to 0.45 V) of (1) 10 mmol dm<sup>-3</sup> AB (2) 10 mmol dm<sup>-3</sup> DMAB and (3) 8 mmol dm<sup>-3</sup> NaBH<sub>4</sub> at gold microdisk in 1 mol dm<sup>-3</sup> NaOH at 100 mV s<sup>-1</sup>.

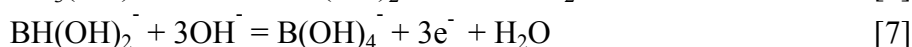
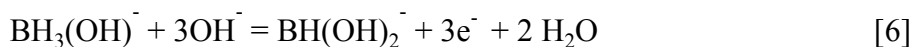


Ab initio molecular orbital order modelling of the DMAB reaction pathway has been investigated [6,29] where the reaction intermediate was considered to be 3 or 5 coordinate. From this work it appears that during the oxidation process the reaction pathway exhibits a potential shift following the third electron transfer which indicates that the intermediate at this point is more stable than the others in the mechanism. The suggested reaction pathway for AB and DMAB oxidation may be represented by equations 4-5 or 6-7 depending on whether the aforementioned intermediate exists as a 5 coordinate or 3 coordinate species, respectively. The techniques employed in this study cannot reveal the identity of these species or the coordination type. Further analysis of these systems such as those proposed in [20] is required to identify the intermediates involved for this technologically relevant system.

*Reaction pathway:*



or



### Conclusions.

Microelectrodes have been utilised to analyse the oxidation of DMAB and AB and the results compared with borohydride oxidation. As in the case of DMAB two oxidation waves have been observed for AB. Data was acquired at microelectrodes to independently determine the diffusion coefficient for the AB. Using the D value determined the coulomb number assigned to both of the oxidation waves was three. The six-electron oxidation reaction is dependent on the concentration of AB in 1 M NaOH. At concentrations greater than 40 mmol dm<sup>-3</sup> AB oxidation also evolves hydrogen gas and the coulomb number is less than six. AB and borohydride exhibit simpler voltammograms than DMAB. The introduction of dimethylamine independently appears to complicate the reaction process for AB at the surface of the electrode particularly for the second oxidation wave.

### Acknowledgments

The authors thank the Irish Research Council for Science, Engineering and Technology (IRCSET) for financial support.

### References

1. F. Pearlstein and R.F. Weightman, *Plat.*, **60**, 474 (1973)
2. M. Lelental, *J. Catal.*, **32**, 429 (1974).
3. C.D. Iacovangelo, *J. Electrochem. Soc.*, **138**, 976 (1991).
4. J.C. Patterson, C. Ni Dheasuna, J. Barrett, T.R. Spalding, M. O'Reilly, X.Jiang and G.M. Crean, *Appl. Surf. Sci.*, **91**, 124 (1995)
5. A. Chiba, H. Haijima and K. Kobayashi, *Surf. Coat. Tech.*, **169-170**, 104 (2003).

6. T. Homma, A. Tamaki, H. Nakai and T. Osaka, *J. Electroanal. Chem.*, **559**, 131 (2003).
7. A. Sargent, O. Sadik and L. Matienzo, *J. Electrochem. Soc.*, **148**, C257 (2001).
8. Y. Yamauchi, T. Yokoshima, H. Mukaibo, M. Tezuka, T. Shigeno, T. Momma, T. Osaka and K. Kuroda, *Chem. Lett.*, **33**, 542 (2004).
9. J.M. Izaki and T. Omi, *J. Electrochem. Soc.*, **144**, L3 (1997).
10. M. Izaki and J. Katayama, *J. Electrochem. Soc.*, **147**, 210 (2000).
11. M. Chigane, M. Izaki, T. Shinagawa and M. Ishikawa, *Electrochem. Solid-State Lett.*, **7**, D1 (2004).
12. T. Osaka, N. Takano, T. Kurokawa, T. Kaneko and K. Ueno, *Surf. Coat. Tech.*, **169-170**, 124 (2003)
13. A. Gutowska, L. Li, Y. Shin, C.M. Wang, X.S. Li, J.C. Linehan, R.S. Smith, B.D. Kay, B. Schmid, W. Shaw, M. Gutowski and T. Autrey, *Angew. Chem. Int. Ed.*, **44**, 3578, (2005)
14. Y. Chen, J.L. Fulton, J.C. Linehan and T. Autrey, *J. Am. Chem. Soc.*; **127**, 3254 (2005)
15. E. Gyenge, *Electrochim. Acta*, **49** 965 (2004)
16. Z.P. Li., B.H. Liu, K. Arai, K. Asaba, S. Suda, *J. Power Sources*, **126**, 28 (2004)
17. B.H. Liu, Z.P. Li and S. Suda, *J. Electrochem. Soc.*, **150**, A398 (2003)
18. A. Verma and S. Basu, *J. Power Sources*, **145**, 282 (2005)
19. B.H. Liu, Z.P. Li, K. Arai, S. Suda, *Electrochim. Acta* **50**, 3719 (2005)
20. E.J. O'Sullivan, *Advances in Electrochemical Science and Engineering*, Volume 7, R.C. Alkire and D.M. Kolb Editors, p. 225 Wiley, New York, 2001.
21. D. Pletcher, *Microelectrodes: Theory and Application*, sect. 1. M. I. Montenegro, M. A. Queirós and J. L. Daschbach, Editors, Kluwer Academic Publishers, Dordrecht, 1990.
22. L.C. Nagle and J.F. Rohan, *Electrochem. Solid-State Lett.*, **8**, C77 (2005)
23. M.V. Mirkin, H. Yang and A.J. Bard, *J. Electrochem. Soc.*, **139**, 2212 (1992).
24. J.A. Gardiner and J.W. Collat, *J. Am. Chem. Soc.*, **87**, 1692 (1965).
25. J.A. Gardiner and J.W. Collat, *Inorg. Chem.*, **4**, 1208 (1965).
26. L.D. Burke and B.H. Lee, *J. Appl. Electrochem.*, **22**, 48 (1992)
27. G. Denault, M. Mirkin and A.J. Bard, *J. Electroanal. Chem.*, **308**, 27 (1991).
28. Y. Okinaka, *J. Electrochem. Soc.*, **120**, 739 (1973).
29. T. Homma, H. Nakai, M. Onishi and T. Osaka, *J. Phys. Chem. B*, **103**, 1774 (1999).